# Synthesis and characterization of $Cd_{1-x}Pb_xSe$ ($0 \leq x \leq 1$) thin films deposited by chemical bath for photovoltaic application

D. A. Adu-Boadu [a], M. Paal [a], M. B. Mensah [b], I. Nkrumah [a,*], R. Y. Tamakloe [a], F. K. Ampong [a], R. K. Nkum [a], F. Boakye [a]
[a] *Department of Physics, Kwame Nkrumah University of Science and Technology, Kumasi, Ghana*
[b] *Department of Chemistry, Kwame Nkrumah University of Science and Technology, Kumasi, Ghana*

$Cd_{1-x}Pb_xSe$ ($0 \leq x \leq 1$) thin films with values of x = 0, 0.2, 0.4, 0.5 and 1, have been deposited by chemical bath technique for photovoltaic application. The deposition temperature, time and pH of the reactive solutions were 80 °C, 150 min and 11 respectively. The XRD results confirmed the polycrystalline nature of all the films. It also showed that all the films exist in face centered cubic structures. There were no pure phases of CdSe and PbSe identified in the XRD results of the ternary compounds. The average grain sizes determined for each sample were found to be between 10.503, and 14.113 nm and their corresponding lattice constants were found to range from 0.605 and 0.6128 nm. The dislocation densities were also found to decrease with increasing lead content and ranged between $9.065\times10^{14}$ and $5.021\times10^{14}$ $m^2$. The EDX analysis conducted confirmed the deposition of $Cd_{1-x}Pb_xSe$ thin films. It was also observed that with the increase in lead content in the CdSe crystal lattice host, the grain sizes and intergranular spacing increased. The band gaps were found to decrease with increasing lead content from 1.80 to 1.38 eV, which are well within the optimum range for photovoltaic application.

(Received March 11, 2025; Accepted July 8, 2025)

*Keywords:* Chalcogenide, Cadmium lead selenide, Solid solution, Alloy, Dislocation density

## 1. Introduction

Research on thin films, which are based on phenomena that are unique to the thickness, geometry, and structure of the film, has either directly or indirectly advanced the frontiers of solid state physics. Thin film research has increased dramatically, partly because of its wide range of applications in electronics, optics, space science, aircraft, defense, and other industries [1]. The numerous discoveries are in the form of active and passive devices [2], sensor and laser materials [3-4], photoresistors [5], solar cells and thin film transistors [6], thermoelectric devices [7], optical filters and optical recording materials [8], gamma ray detectors [9], photoluminescent devices [10], and more recently, as infrared emitters [11].

The synthesis of semiconductor thin film materials as absorber layers for photoelectrochemical solar cells, which convert solar energy to electrical energy, has received a lot of attention recently [12]. This is because the world needs reliable alternative energy sources that aren't too expensive, to help meet its energy demands. Among these materials include the highly researched and the highly light sensitive binary lead and cadmium chalcogenides which include PbSe and CdSe. Many unique properties of the compounds consist of a direct band gap that corresponds with the solar spectrum, a high absorption coefficient in the visible and infrared regions, favourable electrical and magnetic properties [13–14], and the ease of doping to produce n-type or p-type conductivity. These properties as well as lattice constants, and their thermoelectric power can be controlled by controlling the composition of the materials [15].

Despite the successes achieved in the fabrication of binary compounds, ternary compounds of cadmium lead chalcogenides have garnered a lot of interest from both an applied and fundamental

* Corresponding author: inkrumah.sci@knust.edu.gh
https://doi.org/10.15251/CL.2025.227.603

standpoint, with the suggestion that, alloying of Pb into the crystal lattice of CdSe has significant effect on the electrical activity and band gap of these materials [13]. These ternary group II-IV-VI semiconductor materials find their uses in photoelectrochemical (PEC) solar cells, solar control coatings, optoelectronics, and gas and humidity sensors [16]. CdPbS and CdPbSe are two important ternary compounds from the group. Between the two, quite extensive research work has been carried out on CdPbS because of the relative ease in the synthesis of the compound [17].

Till date, different deposition techniques have been employed to deposit various semiconducting materials. Among these techniques include, electrodeposition [18], successive ionic layer adsorption and reaction (SILAR), physical vapor deposition [19], cathodic electrodeposition [20], vacuum evaporation, thermal evaporation [21], molecular beam epitaxy, pulsed laser deposition method [22], sonochemistry, electrochemical atomic layer epitaxy, microwave heating [23] and chemical bath deposition method [24].

Chemical bath deposition technique, which has currently gained significance because of its low cost, simplicity, potential of yielding uniform and high-quality films, ease of substrate choices, enabling multiple sample deposition [25] and convenient for large area deposition [24] has been used in time past to deposit CdPbSe thin films of varying compositions.

In this work, we have deposited cadmium lead selenide ($Cd_{x-1}Pb_xSe$) thin films of different compositions using chemical bath deposition technique at a relatively high temperature of 80 $^oC$ and with ammonia ($NH_3$) as complexing agent. The structural, surface morphology, chemical composition and optical properties of the as-deposited thin films were investigated and the results reported.

## 2. Materials and methods

### 2.1. Substrate preparation

Microscopic glass substrates were prepared to remove any dirt and possible grease on their surfaces for better adherence and uniformity of the thin films by washing them with ordinary water and soap and then rinsing with deionized water. They were then soaked in nitric acid ($HNO_3$) and placed in a sonicator for 10 min and at a temperature of 30 $^oC$ to remove all the dirt and possible grease on them. They were again washed or rinsed with deionized water. The substrates were further soaked in ethanol ($CH_3CH_2OH$) contained in relatively large tubes and were placed in the sonicator for about 10 min to neutralize excess acid that might be on them. The substrates were finally rinsed with deionized water and dried under ambient conditions.

### 2.2. Source of materials

Every chemical employed in this project was of analytical quality. 0.25 M cadmium acetate dihydrate, [$Cd(CH_3COO)_2$. $2H_2O$], was the source of the cadmium ions. 0.25 M sodium selenosulphite, [$Na_2SeSO_3$] also served as selenium ions source, lead nitrate [$Pb(NO_3)_2$] of 0.25 M was the lead ions source, and 25 % Ammonia ($NH_3$) as complexing agent as well as to enhance the pH of the aqueous solutions.

Through a process called refluxing, sodium selenosuphite solution with concentration 0.25 M was prepared. About 7.48 g of sodium sulphite ($Na_2SO_3$) was put into a 250 ml volumetric flask after being dissolved in deionized water. A final volume of 250 ml of $Na_2SO_3$ was obtained by adding deionized water. The solution was then well shaken to obtain a uniform sodium sulphite solution. After that, it was heated to a constant temperature of 90 $^oC$ while ensuring continuous stirring. At 90 $^oC$, 4.89 g of 99.9 % pure elemental selenium powder was incorporated into the mixture. The mixture was then heated for 6 h while being continuously stirred to produce $Na_2SeSO_3$ solution. Afterwards, the resulting solution was left to cool before being filtered to yield a clear $Na_2SeSO_3$ solution.

### 2.3. Deposition of $Cd_{x-1}Pb_xSe$ ($0 \leq x \leq 1$)

The chemical bath preparation involved the mixing of appropriate amounts of cadmium acetate, lead nitrate, ammonia and sodium selenosulphite solutions in the stoichiometric ratio of $(1 - x)$: $x$: 1 and complexed with equal volume of ammonia in a 100 ml beaker. After adding 10 ml

of sodium selenosulphite ($Na_2SeSO_3$), some quantity of deionized water was added for a final volume of 80 ml to be obtained. The pH of the solution was 11. The slides which had undergone chemical treatment were vertically immersed in the reaction beaker. After that, the beaker was submerged in an 80 °C constant temperature water bath and constantly stirred. The films were formed on the slides after 150 min, at which point the slides were taken out, washed with deionized water, and allowed to dry naturally prior to film characterization. Films with compositions $Cd_{1-x}Pb_xSe$ were obtained for composition parameter x = 0, 0.2, 0.4, 0.5 and 1.

## 3. Results and discussion

### 3.1. X-ray diffraction studies

An X-ray diffraction examination was performed to ascertain the orientation and crystal structural properties of the deposited films. The X-ray diffractometer employed was the Empyrean Series 2 PANalytical (WP_20140702_009). The source of the monochromatic radiation was CuKα (1.54060 Å). With a step size of 0.2 º and a 2θ range of 5 to 80 º, the diffractometer was run in the step scan mode. The X-ray tube's operational voltage and current were 45 kV and 40 mA, respectively. The Empyrean Series 2 PANalytical XRD device was operated on the Bragg-Brentano geometry. XRD data were analyzed with Origin software package. Identification of the peaks were done by matching the diffractograms and comparing the d-spacing values obtained with the International Center for Diffraction Data (ICDD) standards and the results are displayed in Figure 1.

At the given experimental conditions, the existence of several peaks for all the samples indicate the polycrystalline nature of the films. Films of x = 0, 0.4, 0.5 show very prominent and well-defined peaks due to reflections from (111), (002), and (022) planes. It can be observed that with x = 0.2, the (002) plane is hardly visible even though the XRD pattern confirms the existence of that phase. As the concentration of lead increased, the peak at the (002) plane becomes the most prominent and the preferred orientation instead of the (111). The presence of other well-defined peaks was due to reflections from (113), (222), (004), (024), and (224) planes. XRD studies conducted also showed that all the samples exist in the face centered cubic (zinc blende) structures. There were no pure phases of CdSe and PbSe identified in the ternary compounds. The unindexed peaks represent impurity phases.

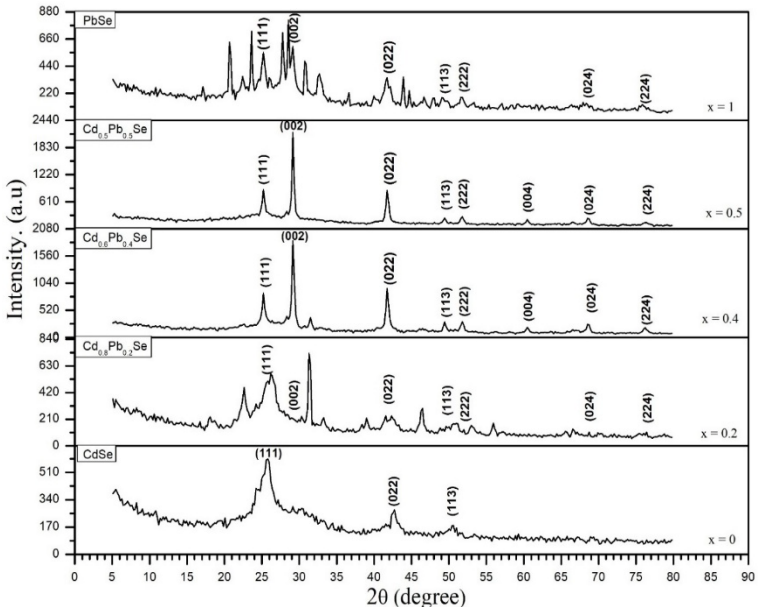


*Fig. 1. Stacked XRD Diffractograms for $Cd_{1-x}Pb_xSe$ (0≤ x ≤ 1) thin films.*

Lattice constants, $a_{hkl}$ for the cubic structures were calculated using the equation below [26]:

$$a_{hkl} = d_{hkl}\sqrt{h^2 + k^2 + l^2} \quad (1)$$

The $a_{hkl}$ values for each sample are recorded in Table 1.

**3.2. Average grain size and dislocation density**

Debye-Scherrer's formular was used to determine the average grain size for each sample and is given by the relation [27];

$$D = \frac{K\lambda}{\beta Cos\theta_,} \quad (2)$$

where, D is average crystallite size, λ is wavelength of X-ray used as the primary beam of CuKα (λ = 1.54060 Å), β is full width at half maxima of the most intense peak (FWHM) in radians, θ is Bragg's angle, and K is a constant (K = 0.9). The average crystallite sizes were determined for x = 0, 0.2, 0.4, 0.5 and 1, based on the XRD data.

Williamson and Smallman's formular was used to calculate the dislocation density (δ) which from the average crystallite size, D, gives the number of defects present [24].

$$\delta = \frac{1}{D^2} \quad (3)$$

The average crystallite sizes as well as the dislocation densities $\delta$ computed for each sample are recorded in Table 1.

*Table 1. Lattice constants, average grain sizes and dislocation densities for $Cd_{1-x}Pb_xSe$ samples (x = 0, 0.2,0.4, 0.5, 1).*

| Sample | hkl | 2θº | d-spacing | Lattice constant $a_{hkl}$ (nm) | Average crystallite size, (nm) | Dislocation density, δ /m$^2$ |
|---|---|---|---|---|---|---|
| CdSe | 111 | 25.480 | 3.49297 | 0.6050 | 10.503 | $9.065\times10^{14}$ |
| | 022 | 29.505 | 3.02500 | | | |
| | 113 | 49.957 | 1.82414 | | | |
| $Cd_{0.8}Pb_{0.2}Se$ | 111 | 25.247 | 3.52472 | 0.6050 | 13.998 | $5.103\times10^{14}$ |
| | 002 | 29.233 | 3.05250 | | | |
| | 022 | 41.817 | 2.15844 | | | |
| | 113 | 49.447 | 1.84073 | | | |
| | 222 | 51.836 | 1.76236 | | | |
| | 024 | 68.704 | 1.36512 | | | |
| | 224 | 76.359 | 1.24618 | | | |
| $Cd_{0.6}Pb_{0.4}Se$ | 111 | 25.247 | 3.52472 | | 14.117 | $5.018\times10^{14}$ |
| | 002 | 29.233 | 3.05250 | 0.6105 | | |
| | 022 | 41.817 | 2.15844 | | | |
| | 113 | 49.447 | 1.84073 | | | |
| | 222 | 51.836 | 1.76236 | | | |
| | 004 | 60.623 | 1.52625 | | | |
| | 024 | 68.704 | 1.36512 | | | |

| Sample | hkl | 2θ° | d-spacing | Lattice constant $a_{hkl}$ (nm) | Average crystallite size, (nm) | Dislocation density, δ /m$^2$ |
|---|---|---|---|---|---|---|
| | 224 | 76.359 | 1.24618 | | | |
| $Cd_{0.5}Pb_{0.5}Se$ | 111 | 25.247 | 3.52472 | | 14.117 | $5.018\times10^{14}$ |
| | 002 | 29.233 | 3.05250 | 0.6105 | | |
| | 022 | 41.817 | 2.15844 | | | |
| | 113 | 49.477 | 1.84073 | | | |
| | 222 | 51.836 | 1.76236 | | | |
| | 004 | 60.623 | 1.52625 | | | |
| | 024 | 68.704 | 1.36512 | | | |
| | 224 | 76.359 | 1.24618 | | | |
| PbSe | 111 | 25.150 | 3.53800 | | 14.113 | $5.021\times10^{14}$ |
| | 002 | 29.121 | 3.06400 | 0.6128 | | |
| | 022 | 41.653 | 2.16657 | | | |
| | 113 | 49.477 | 1.84073 | | | |
| | 222 | 51.627 | 1.76900 | | | |
| | 024 | 68.410 | 1.37026 | | | |
| | 224 | 76.359 | 1.24618 | | | |

The calculated lattice constants agree with standard values except for x = 0.2 which differs by 0.0055 nm (0.055 Å) from reported standard value of 0.6105 nm (6.105 Å). They are also similar to those reported by [28]. There was a marginal increase in the lattice constant with increasing concentration of lead, except that it remained constant for x = 0.4 and x = 0.5. The dislocation density generally decreased with increasing concentration of the dopant, Pb, except that it remained the same for x = 0.4 and 0.5. The decrease in dislocation density is good because the fabrication of quality thin films for photovoltaic devices requires as a matter of necessity, reduction in surface roughness as well as the dislocation density [22]. The graph of grain size versus percentage doping is shown in Figure 2.

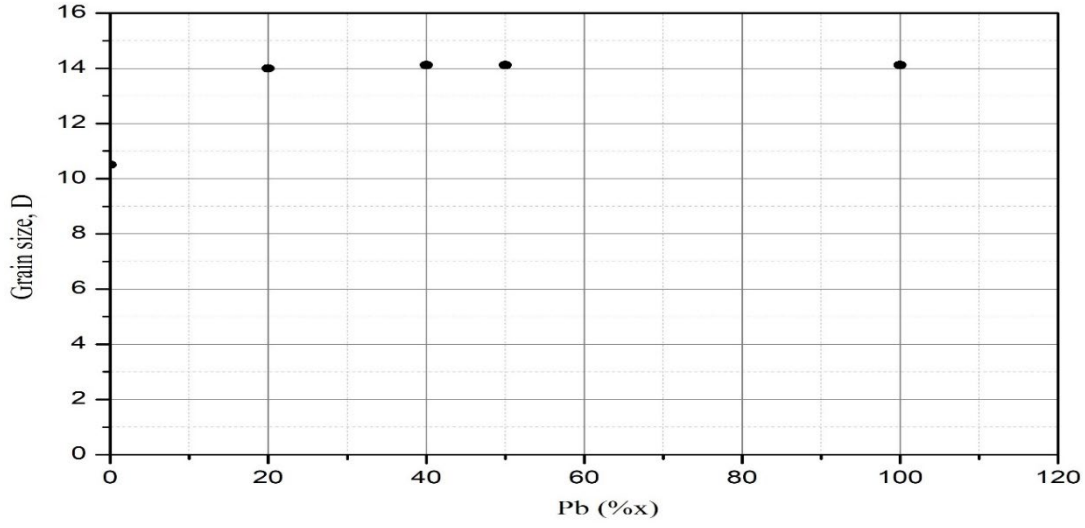


*Fig. 2. Graph of grain size versus percentage doping.*

Since the ionic radius of lead ($Pb^{2+}$) which is 1.19 Å (0.119 nm), is greater than that of cadmium ($Cd^{2+}$) which is 0.95 Å (0.095 nm), incorporating lead into the crystal lattice of cadmium increases the crystal size and the average crystallite size would increase [29]. Grain size significantly

increased when the lead content rose from 0 to 20%, according to the graph. This was followed by a marginal increase in crystallite size as the concentration increased from 20 to 50 %. The calculated average crystallite sizes were found to differ from those reported by [28].

### 3.3. SEM and EDAX analysis

The surface morphology as well as the chemical compositions of the composites of $Cd_{1-x}Pb_xSe$ (x = 0, 0.2, 0.4, 1) thin films were examined using the Zeiss SmartEDX apparatus operated at nominal electron beam voltage of 15 kV. The SEM images and EDX results are displayed in Figures 3, 4, 5, and 6. The presence of elements Cd, Pb and Se confirms the deposition of thin films of CdPbSe. Also, the presence of Si, O and other impurity elements might have resulted from the substrate and chemicals used.

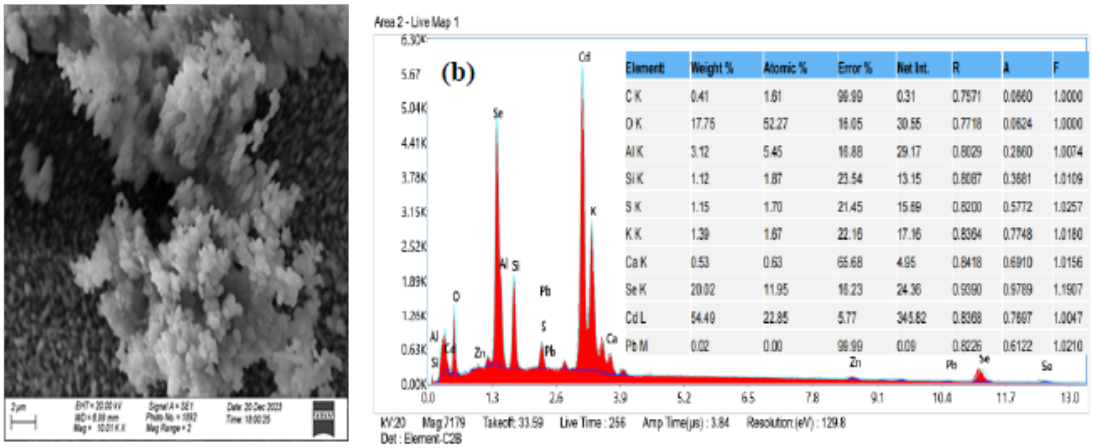


*(a)* *(b)*

*Fig. 3. (a) SEM micrograph and (b) EDX spectrum of $Cd_{1-x}Pb_xSe$ (x = 0).*

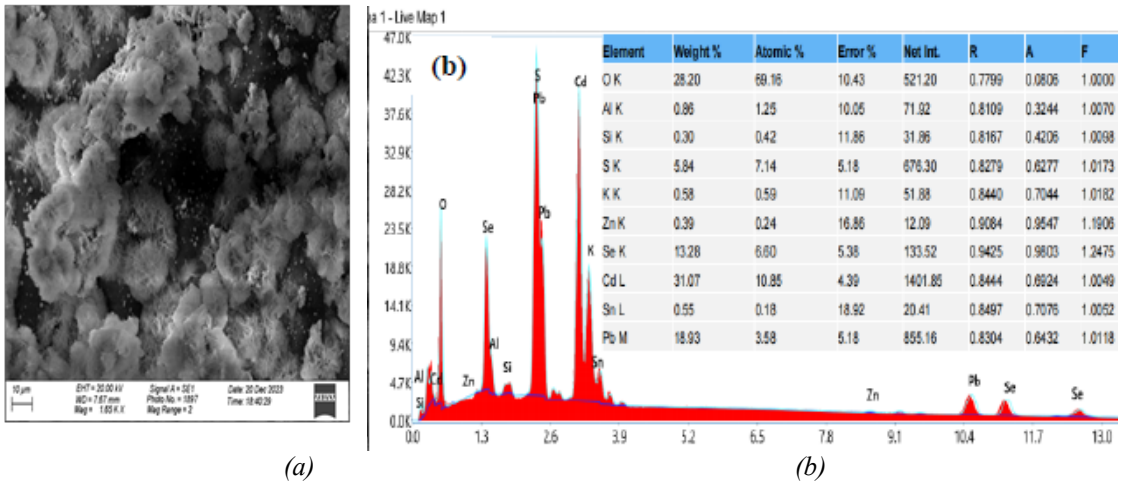


*(a)* *(b)*

*Fig. 4. (a) SEM micrograph and (b) EDX spectrum of $Cd_{1-x}Pb_xSe$ (x = 0.2)*

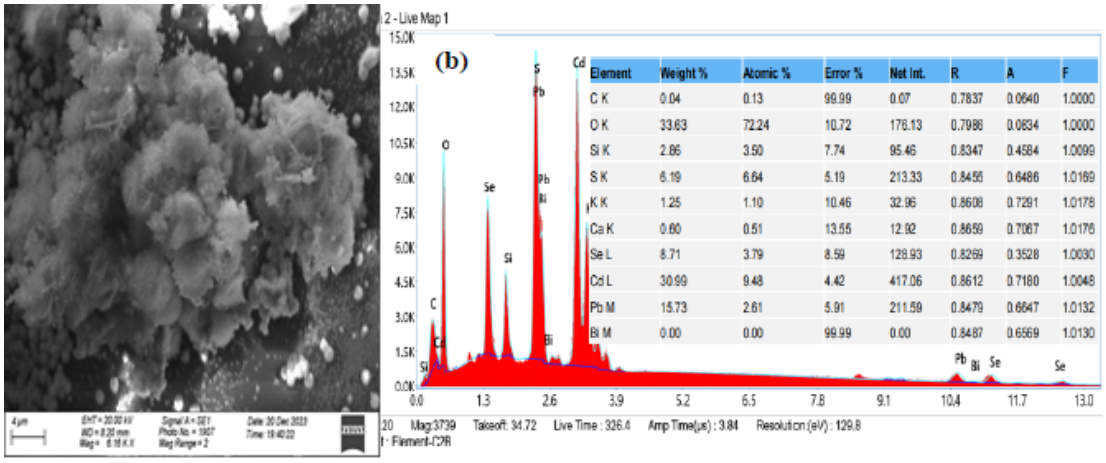


*(a)* *(b)*

*Fig. 5. (a) SEM micrograph and (b) EDX Spectrum of $Cd_{1-x}Pb_xSe$ (x = 0.4)*

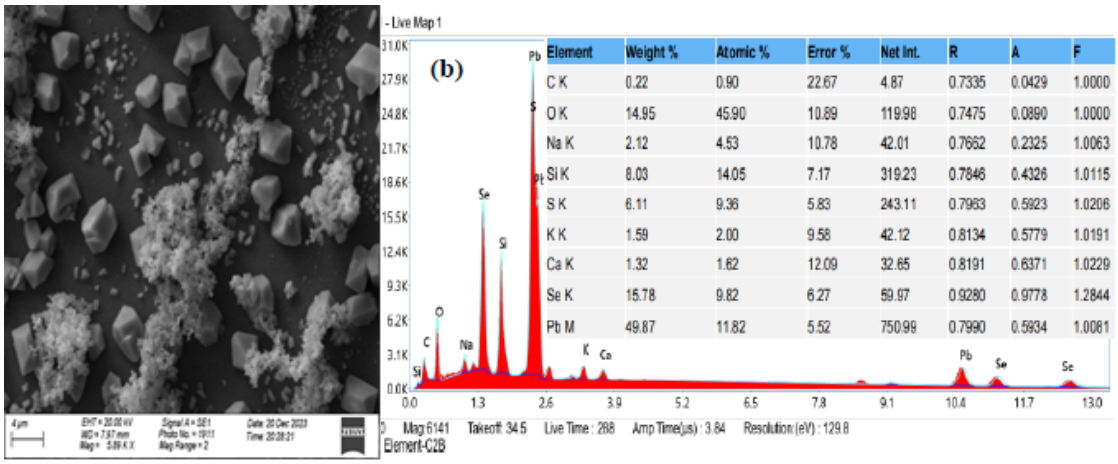


*(a)* *(b)*

*Fig. 6. (a) SEM micrograph and (b) EDX Spectrum of $Cd_{1-x}Pb_xSe$ (x = 1).*

From the micrographs, there is evidence of the polycrystalline nature of all the samples as confirmed by the XRD studies. The surfaces are rough with clearly defined spherical grains except for sample x = 1 (PbSe), which looks like fragmented cubes. For x = 0 (CdSe), the grains are small and compact, covering the whole substrate surface. The images further reveal spots of cluster of grains forming in all the samples. Generally, it can be inferred that the deposition mechanism of the films was predominantly ion-by-ion mechanism. Further comparative observational studies also show that, the grain sizes increased and the intergranular spacing additionally increased in tandem with a rise in the volume concentration of Pb in confirmation with what had earlier been reported by Patil et al. [28]. From the results, there was no evidence of cracks and holes making the films suitable for photovoltaic application.

### 3.4. Optical studies

#### *3.4.1. Determination of the optical band gap*

The Biobase, BK-D560 spectrophotometer with a wavelength range of 190-1100 nm was used to obtain the absorbance-wavelength data of the $Cd_{1-x}Pb_xSe$ ($0 \leq x \leq 1$) thin films. The band gaps were found by treating the data obtained mathematically using the Stern's relation cited in Puzer et al. [30]:

$$(Ahv) = [k(hv - E_g)]^{\frac{n}{2}} \quad (4)$$

where A is absorbance, h$v$ is the energy of the incident light photon (h is Planck's constant and $v$ is photons' frequency), $E_g$ is the optical energy gap, n is an integer whose value depends on the transition type. For direct transition n = 1 and for indirect transition n = 4. Both CdSe and PbSe are direct band gap materials and hence their mixed would be assumed to also have a direct band gap, hence n = 1.

$(Ahv)^2$ is plotted as a function of h$v$ in Figures 7–11. In order to determine the band gap, the linear portion of the graph is fitted using a line of best fit that intersects the h$v$ axis [27].

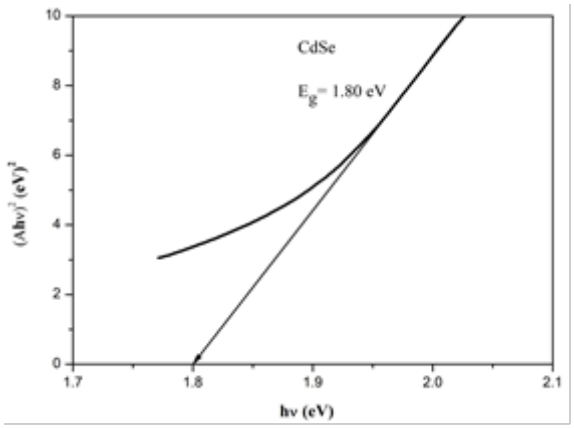


*Fig. 7. A plot of $(Ahv)^2$ vrs hv for x = 0.*

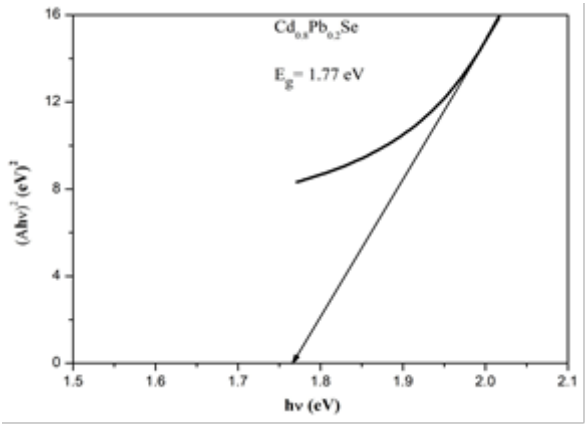


*Fig. 8. A plot of $(Ahv)^2$ vrs hv for x = 0.2.*

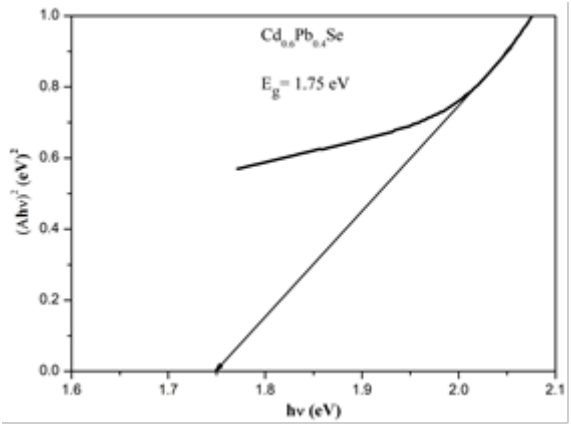


*Fig. 9. A plot of $(Ahv)^2$ vrs hv for x = 0.4.*

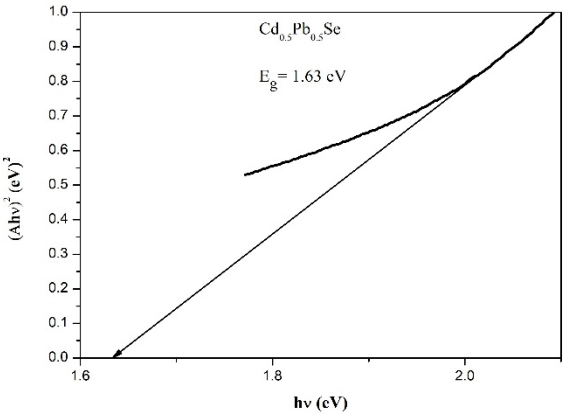


*Fig. 10. A plot of $(Ahv)^2$ vrs hv for x = 0.5.*

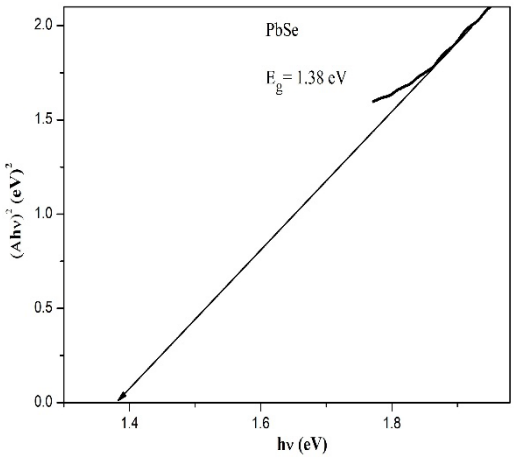


*Fig. 11. A plot of $(Ahv)^2$ vrs hv for x = 1.*

From Figures 7 – 11, the estimated band gaps of $Cd_{1-x}Pb_xSe$ for x = 0, 0.2, 0.4, 0.5 and 1 are 1.80, 1.77, 1.75, 1.63 and 1.38 eV respectively. It was noted that there was a decrease in the band gaps of the samples as the x-parameter increased. This is because the Pb has a lower band gap. The graph of band gap plotted against composition parameters is as shown in Figure 12.

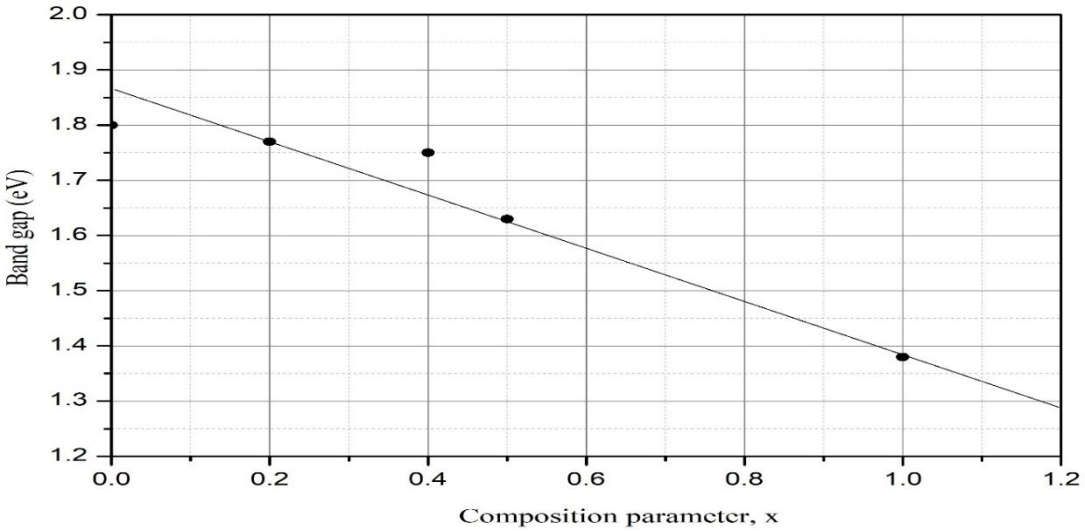


*Fig. 12. Graph of band gap versus composition parameter, x.*

From the graph, there is an observed linear relationship between the band gap and composition parameter, x, and shows that as composition parameter increases, the band gap decreases.

From the EDX and optical absorption studies, the results of the analysis of the compositions of only the major elements for each sample of $Cd_{1-x}Pb_xSe$ ($0 \leq x \leq 1$) and their respective band gaps are reported in Table 2.

*Table 2. Compositional analysis and energy band gap of $Cd_{1-x}Pb_xse$ thin films.*

| Composition parameter, x | Sample composition | Bath content % | | | Atomic % | | | Band gap ($E_g$) eV |
|---|---|---|---|---|---|---|---|---|
| | | Cd | Pb | Se | Cd | Pb | Se | |
| x = 0.0 | CdSe | 50.0 | 0.0 | 50.0 | 65.7 | 0.0 | 34.3 | 1.80 |
| x= 0.2 | $Cd_{0.8}Pb_{0.2}Se$ | 40.0 | 10.0 | 50.0 | 51.6 | 17.0 | 31.4 | 1.77 |
| x = 0.4 | $Cd_{0.6}Pb_{0.4}Se$ | 30.0 | 20.0 | 50.0 | 59.7 | 16.4 | 23.9 | 1.75 |
| x = 0.5 | $Cd_{0.5}Pb_{0.5}Se$ | 25.0 | 25.0 | 50.0 | No EDX analysis conducted | | | 1.63 |
| x = 1.0 | PbSe | 0.0 | 50.0 | 50.0 | 0.0 | 54.6 | 45.4 | 1.38 |

## 4. Conclusion

Successful deposition of $Cd_{1-x}Pb_xSe$ ($0 \leq x \leq 1$) with specific values of x = 0, 0.2, 0.4, 0.5 and 1 for photovoltaic application has been achieved. A relatively less expensive deposition technique, chemical bath, was employed for the deposition. The optimum conditions for the depositions were 80 $^oC$, 150 min and pH, 11. The XRD results confirmed that all of the films were polycrystalline and exist as face centered cubic structures. The average grain size was found to increase for increasing lead content and ranged between 10.503, and 14.113 nm. The dislocation density also decreased with increasing lead content and were found to be between $9.065 \times 10^{14}$ and $5.021 \times 10^{14}$ $m^2$. SEM analysis conducted on the samples showed that the surfaces of all the samples were rough, and the grains were spherical in shape and EDX confirmed the deposition of CdPbSe. The band gaps of CdSe, $Cd_{0.8}Pb_{0.2}Se$, $Cd_{0.6}Pb_{0.4}Se$, $Cd_{0.5}Pb_{0.5}Se$ and PbSe were found to be 1.80, 1.77, 1.75, 1.63 and 1.38 eV, respectively. The bang gaps are within the optimum range of band gaps for absorber materials and thus, make the films favourable for use as absorber layer for photovoltaic application.

## References

[1] S. Vyas, Johnson Matthey, Technology Review, **64**(2), 202. (2020); https://doi.org/10.1595/205651320X15694993568524
[2] F. Catania, H.S. Oliveira, P. Lugoda, G. Cantarella, N. Münzenrieder, Journal of Physics D: Applied Physics, **55**(32), 323002. (2022); https://dx.doi.org/10.1088/1361-6463/ac6af4
[3] T.A. Truong, T.K. Nguyen, H. Zhao, N.K. Nguyen, T. Dinh, Y. Park, H.P. Phan, Nano.Micro Small, **18**(4), 2105748. (2022); https://dx.doi.org/10.1088/1361-6463/ac6af4
[4] P. Priyadarshini, S. Das, R. Naik, Royal Society of Chemistry, **12**(16), 9611. (2022); https://doi.org/10.1039/D2RA00771A
[5] M.Y. Thabit, N. M. Kaawash, S. Begum, D.I. Halge, V.N. Narwade, P.S. Alegaonkar, K.A. Bogle, In Journal of Physics, **2426**(1), 012004 (2023); https://doi.org/10.1088/1742-6596/2426/1/012004
[6] Y. Shen, M. Zhang, S. He, L. Bian, J. Liu, Z. Chen, Y. Yan, Journal of Materials Chemistry **12**(35), 13708. (2024); https://doi.org/10.1039/d4tc01392a
[7] S. Irfan, Z. Yan, S.B. Khan, Materials Science for Energy Technologies, **7**, 350. (2024); https://doi.org/10.1016/j.mset.2024.06.002
[8] A.S. Hassanien, I.M.E. Radaf, A.A. Akl, Journal of Alloys and Compounds, **849**, 156718. (2020); https://doi.org/10.1016/j.jallcom.2020.156718
[9] J.M.C.F. da Silva, N.F.V. Borrero, A. de Morais, J.N. de Freitas, M.F. das Chagas, Next Energy, **6**, 100192. (2025); https://doi.org/10.1016/j.nxener.2024.100192
[10] M. Khan, G.A. Nowsherwan, R. Ali, M. Ahmed, N. Anwar, S. Riaz, J.R. Choi, Molecules, **28**(24), 7963 (2023); https://doi.org/10.3390/molecules28247963
[11] S. Liang, F. Xu, W. Li, W. Yang, S. Cheng, H. Yang P. Jiang, Applied Thermal Engineering, **232**, 121074. (2023); https://doi.org/10.1016/j.applthermaleng.2023.121074
[12] M.A. Bilya, A. Nabok, Y.P. Purandare, A.E. Alam, I. M. Dharmadasa, Energies, **17**(2), 406 (2024); https://doi.org/10.1002/aenm.202402640
[13] H.H. Gullu, M. Isik, O. Surucu, N.M. Gasanly, M.E.H.M.E.T. Parlak, Materials Science in Semiconductor Processing, **123**, 105559 (2021); https://doi.org/10.1016/j.mssp.2020.105559
[14] M.C. Gupta, J. T. Harrison, M.T. Islam, Materials Advances, ***2***(10), 3133-3160. (2021); https://doi.org/10.1039/D0MA00965B
[15] S.D. Delekar, P. P. Hankare, Materials Science Forum **764,** 293. (2013); https://doi:10.4028/www.scientific.net/MSF.764.29
[16] R.S. Devika, P. Vengatesh and T.S. Shyju, Materials Today: Proceedings (2023); https://doi.org/10.1016/j.matpr.2023.04.113
[17] S.B. Nair, A. Abraham, B. Pradeep, T. Shripathi, V. Ganesan, R.R. Philip, AIP Conference Proceedings, **1620**, 511. (2014); https://doi.org/10.1063/1.4898289
[18] S. Saha, M. Johnson, F. Altayaran, Y. Wang, D. Wang, Q. Zhang, Electrochem, **1**(3), 286-321 (2020); https://doi.org/10.3390/electrochem1030019
[19] T. Nimalan, M. Begam, Int. J. Thin. Fil. Sci. Tec, **13**(1), 59-66. (2024). https://doi.org/10.1016/j.jmrt.2022.10.064
[20] S. Sen, A. Chatterjee, D. Ramakanth, S. Singh, P.K. Maji, Progress in Organic Coatings, **190**, 108387 (2024); https://doi.org/10.1016/j.porgcoat.2024.108387
[21] B. Janarthanan, C. Thirunavukkarasu, S. Maruthamuthu, M.A. Manthrammel, M. Shkir, S. AlFaify, C. Park, Journal of Molecular Structure **1241**, 130606 (2021); https://doi.org/10.1016/j.molstruc.2021.130606
[22] A.J. Haider, T. Alawsi, M.J. Haider, Opt Quant Electron, **54**, 488 (2022); https://doi.org/10.1007/s11082-022-03786-6
[23] A.S. Patil, A.V. Patil, C.G. Dighavkar, V. A. Adole, U.J. Tupe, Chemical Physics Letters, **796** 139555 (2022); https://doi.org/10.1016/j.cplett.2022.139555
[24] C.K. Bandoh, I. Nkrumah, F.K. Ampong, R.K. Nkum, F. Boakye, Chalcogenide Letters **18**(2), 84 (2021).
[25] S. Sengupta, R. Aggarwal, M. Raula, Journal of Material Science Research **38**(1), 142 (2023). https://doi:10.1557/s43578-022-00539-9
[26] S.S. Guruling, N.M. Ramesh, S.S. Dattatraya, P. D. Lalasaheb, Epilayers and

Heterostructures in Optoelectronics and Semiconductor Technology, **4413**, 22 (2001) https://doi:10.1117/12.425434
[27] I. Nkrumah, F.K. Ampong, A. Britwum, M. Paal, B. Kwakye-Awuah, R.K. Nkum, F. Boakye, Chalcogenide Letters, **20**(3), 208 (2023); https://doi.org/10.15251/CL.2023.203.205
[28] S.D. Delekar, M.K. Patil, B.V. Jadhav, K.R. Sanadi, P.P. Hankare, Solar Energy **84**, 396 (2010); https://doi:10.1016/j.solener.2009.12.009
[29] R.S. Patil, H.M. Pathan, T.P. Gujar, C.D. Lokhande, Journal of Materials Science **41**, 5723 (2006); https://doi.org/10.1007/s10853-006-0098-4
[30] D.B. Puzer, I. Nkrumah, F.K. Ampong, M. Paal, E.A. Botchway, R.K. Nkum, F. Boakye, Chalcogenide Letters, **18**(8), 488 (2021); https://doi.org/10.15251/cl.2021.188.481